Structural plasticity of hippocampal mossy fiber synapses as revealed by high-pressure freezing

ARTICLE *in* THE JOURNAL OF COMPARATIVE NEUROLOGY · AUGUST 2012

Impact Factor: 3.23 · DOI: 10.1002/cne.23040 · Source: PubMed

Structural Plasticity of Hippocampal Mossy Fiber Synapses as Revealed by High-Pressure Freezing

Shanting Zhao,[1,3] Daniel Studer,[2] Xuejun Chai,[3] Werner Graber,[2] Nils Brose,[4] Sigrun Nestel,[3] Christina Young,[3] E. Patricia Rodriguez,[5] Kurt Saetzler,[5] and Michael Frotscher[1,3]*

[1]Department for Structural Neurobiology, Center for Molecular Neurobiology Hamburg (ZMNH), University of Hamburg, D-20246 Hamburg, Germany
[2]Institute of Anatomy, University of Bern, CH-3000 Bern, Switzerland
[3]Institute of Anatomy and Cell Biology, University of Freiburg, D-79104 Freiburg, Germany
[4]Department of Molecular Neurobiology, Max Planck Institute for Experimental Medicine, D-37077 Göttingen, Germany
[5]School of Biomedical Science, University of Ulster, Coleraine, BT52 1SA, UK

ABSTRACT

Despite recent progress in fluorescence microscopy techniques, electron microscopy (EM) is still superior in the simultaneous analysis of all tissue components at high resolution. However, it is unclear to what extent conventional fixation for EM using aldehydes results in tissue alteration. Here we made an attempt to minimize tissue alteration by using rapid high-pressure freezing (HPF) of hippocampal slice cultures. We used this approach to monitor fine-structural changes at hippocampal mossy fiber synapses associated with chemically induced long-term potentiation (LTP). Synaptic plasticity in LTP has been known to involve structural changes at synapses including reorganization of the actin cytoskeleton and de novo formation of spines. While LTP-induced formation and growth of postsynaptic spines have been reported, little is known about associated structural changes in presynaptic boutons. Mossy fiber synapses are assumed to exhibit presynaptic LTP expression and are easily identified by EM. In slice cultures from wildtype mice, we found that chemical LTP increased the length of the presynaptic membrane of mossy fiber boutons, associated with a de novo formation of small spines and an increase in the number of active zones. Of note, these changes were not observed in slice cultures from Munc13-1 knockout mutants exhibiting defective vesicle priming. These findings show that activation of hippocampal mossy fibers induces pre- and postsynaptic structural changes at mossy fiber synapses that can be monitored by EM. J. Comp. Neurol. 520:2340–2351, 2012.

INDEXING TERMS: synaptic ultrastructure; hippocampal mossy fibers; CA3 pyramidal cells; long-term potentiation

It has long been assumed that changes in synaptic structure are involved in learning and memory processes (Ramón y Cajal, 1911; Hebb, 1949; Bailey and Kandel, 1993; Trachtenberg et al., 2002; Yang et al., 2009). In long-term potentiation (LTP), a form of synaptic plasticity and model of the mechanisms involved in learning and memory (Nicoll et al., 1988; Bliss and Collingridge, 1993; Whitlock et al., 2006; Bliss et al., 2007; Yang et al., 2008), changes in postsynaptic dendritic spines have been documented (Hosokawa et al., 1995; Buchs and Muller, 1996; Toni et al., 1999; Engert and Bonhoeffer, 1999; Maletic-Savatic et al., 1999; Geinisman, 2000; Matus, 2000; Yuste and Bonhoeffer, 2001; Harris et al., 2003; Matsuzaki et al., 2004; Segal, 2005; Hotulainen and Hoogenraad, 2010). In contrast, it has been difficult to monitor changes in presynaptic axonal boutons although LTP is known to have a presynaptic component (Stevens and Wang, 1994; Emptage et al., 2003; Lauri et al., 2007). Thus, it has remained unclear to what extent presynaptic changes in bouton structure and changes in number and size of postsynaptic spines are related to each other. This holds particularly true for hippocampal

Additional Supporting Information may be found in the online version of this article.

S. Zhao and D. Studer contributed equally to this work.

Grant sponsor: Deutsche Forschungsgemeinschaft; Grant number: SFB 780; Grant sponsor: Swiss National Foundation; Grant number: 3100AO_118394; Grant sponsor: Michael Frotscher is Senior Research Professor of the Hertie Foundation.

*CORRESPONDENCE TO: Michael Frotscher, Department for Structural Neurobiology, Center for Molecular Neurobiology Hamburg (ZMNH), University of Hamburg, Martinistr. 52, D-20246 Hamburg, Germany. E-mail: michael.frotscher@zmnh.uni-hamburg.de

Received August 30, 2011; Revised November 17, 2011; Accepted January 7, 2012
DOI 10.1002/cne.23040
Published online January 11, 2012 in Wiley Online Library (wileyonlinelibrary.com)

mossy fiber (MF) synapses that are generally assumed to exhibit presynaptic expression of LTP (Nicoll and Schmitz, 2005) in an *N*-methyl *D*-aspartate receptor (NMDAR)-independent manner (Harris and Cotman, 1986; but see Kwon and Castillo, 2008; Kerr and Jonas, 2008; Rebola et al., 2008).

Recent studies have shown that long-term experience results in rearrangements of presynaptic MF boutons (MFBs; Galimberti et al., 2006, 2010; Rekart et al., 2007; Routtenberg, 2010). While these studies on MFBs as well as those on spines took advantage of Timm staining of MFs and fluorescence techniques, respectively, and allowed for structural changes to be monitored over time, they were limited by the labeling of only single tissue components at relatively low resolution. Electron microscopy (EM) allows for the simultaneous analysis of all tissue components at high resolution, but it has remained unclear to what extent conventional aldehyde fixation and subsequent dehydration are associated with alterations of the various tissue components. This may be a limitation in studies of rapid, subtle structural changes associated with functional changes at synapses.

Here, high-pressure freezing (HPF; Studer et al., 2001) was applied to study rapid LTP-induced structural changes at MF boutons and their postsynaptic thorny excrescences. High pressure of ≈2,000 bars lowers the freezing point of water, thereby preventing the formation of ice crystals in tissue samples of up to 200 μm thickness and the tissue water is vitrified (Studer et al., 2001). Importantly, following HPF the tissue is not dehydrated in ascending series of ethanol, which in conventional EM may result in tissue shrinkage, but is substituted by methanol or acetone (cryosubstitution).

In the present studies we used slice cultures that were prepared as static cultures (Stoppini et al., 1991) from newborn mice and were incubated in vitro for 14 days to allow for tissue regeneration and removal of debris. Numerous studies have confirmed that the anatomical organization and physiological characteristics of different neuronal types are preserved in an organotypic manner under these conditions (Gähwiler et al., 1997). In particular, MF synapses on the large complex spines or thorny excrescences of identified CA3 pyramidal neurons in slice cultures revealed all fine-structural details as known from studies in perfusion-fixed tissue (Frotscher and Gähwiler, 1988). During incubation, the slices flatten to a thickness of ≈150 μm, allowing them to be placed onto the carriers of a high-pressure freezer. Prior to HPF, in part of the slices chemical LTP (cLTP) was induced with tetraethylammonium (TEA), a blocker of potassium channels. While still exposed to TEA or control medium, the cultures were subjected to HPF to "fix" synaptic structures within less than a second without the use of aldehydes.

We here report that with this approach structural changes in both pre- and postsynaptic compartments of MF synapses could be monitored.

MATERIALS AND METHODS

Animals

Newborn Munc13-1 knockout mutants (Augustin et al., 1999; $n = 12$) and their wildtype littermates ($n = 12$) were used in the present experiments. All animals were maintained in accordance with the animal care guidelines of the National Institutes of Health and the institutional guidelines of the Universities of Freiburg and Hamburg. Genotypes were confirmed by polymerase chain reaction (PCR) analysis of genomic DNA.

Preparation of slice cultures

The present experiments were performed on hippocampal slice cultures ($n = 204$) that were small enough to allow for the tissue to be rapidly frozen without the formation of ice crystals. Under hypothermic anesthesia, newborn animals were decapitated and slice cultures of the hippocampus prepared as described elsewhere (Stoppini et al., 1991). Briefly, the hippocampi were dissected out under sterile conditions and the tissue cut transversely to the longitudinal axis of the hippocampus at 250 μm using a tissue chopper. Slices were placed onto Millipore (Bedford, MA) membranes and transferred to a six-well plate with 1 ml/well nutrition medium (25% heat-inactivated horse serum, 25% Hanks' balanced salt solution, 50% minimal essential medium, 2 mM glutamine, pH 7.2). Slices were incubated as static cultures in 5% CO_2 at 37°C for 14 days with the medium changed every 2 days.

Induction of chemical LTP

For the induction of cLTP, slice cultures were exposed to 25 mM TEA (Sigma, Taufkirchen, Germany) for 10 minutes immediately prior to HPF. This protocol has been shown previously to induce robust cLTP (Suzuki and Okada, 2008). We used this form of LTP because other protocols such as electrical stimulation affect an indeterminate subset of synapses (Hosokawa et al., 1995).

Whole-cell patch clamp recording from CA3 pyramidal neurons

For the recordings, wildtype hippocampal slice cultures were transferred to a recording chamber and continuously superfused at near physiological temperature (30–31°C) with artificial cerebrospinal fluid (ACSF) containing (in mM): 125 NaCl, 25 $NaHCO_3$, 25 glucose, 2.5 KCl, 1.25 NaH_2PO_4, 2 $CaCl_2$, and 1 $MgCl_2$ (equilibrated with 95% O_2 and 5% CO_2) or TEA-ACSF containing (in mM): 25 mM TEACl, 110 NaCl, 25 $NaHCO_3$, 15 glucose, 2.5 KCl, 1.25

NaH_2PO_4, 2 $CaCl_2$, and 1 $MgCl_2$ (equilibrated with 95% O2 and 5% CO_2). The slice cultures were superfused with TEA-ACSF for 10 minutes to induce chemical LTP; before and after cLTP induction normal ACSF was used.

Patch-clamp recordings were made from visually identified CA3 pyramidal neurons using infrared differential interference contrast video microscopy on an upright microscope equipped with a 40× water immersion objective (Zeiss, Oberkochen, Germany) and a video camera (C2400-07, Hamamatsu, Hamamatsu City, Japan).

Patch pipettes were pulled from borosilicate glass tubing (2-mm outer diameter, 1-mm inner diameter) on a Sutter P-87 puller (Sutter Instruments, Novato, CA). The intracellular pipette solution contained (in mM): 135 K-gluconate, 20 KCl, 2 $MgCl_2$, 0.1 EGTA, 10 HEPES, 2 Na_2ATP. The resistance of the filled electrodes was between 4.5 and 5.6 MΩ. All measurements were done in current-clamp at resting membrane potential. The series resistance was fully compensated. Recordings were performed using an Axopatch 200B amplifier (Axon Instruments, Union City, CA).

Spontaneously occurring excitatory postsynaptic potentials (EPSPs) were recorded at the somata of the CA3 pyramidal cells throughout the whole experiment. The amplitude of the EPSPs was measured at control conditions, 10 minutes after TEA treatment, and 15 minutes after TEA treatment. The amplitude of the EPSP was averaged over 20 consecutive EPSPs.

High-pressure freezing

Control cultures from wildtype animals ($n = 48$) and Munc13-1 knockout mice ($n = 36$), and cultures from wildtype animals ($n = 48$) and Munc13-1 knockout mutants ($n = 36$) treated with TEA for 10 minutes were subjected to HPF using an EM PACT 2 (Leica Microsystems, Vienna, Austria). Up to this point the cultures were incubated at 37°C. The following manipulations before freezing lasted less than 1 minute. A sample punch was used to punch out the dentate gyrus together with the CA3 region to fit the tissue to a small membrane carrier (Leica Microsystems). The carrier was inserted in the bayonet pod of the transfer system to hermetically seal the sample. The bayonet pod with carrier and tissue was then loaded into the EM PACT2 and automatically high-pressure frozen in ≈50 ms. During the cooling cycle the sample is cooled by a jet of liquid nitrogen and simultaneously pressurized to 2,000 bars by deformation of the membrane carrier. The sample is cooled with a superficial cooling rate of ≈20,000 K/s, resulting in a cooling rate of 5,000 K/s in the center of the sample. This way the whole sample is cooled to 173 K (−100°C) in about 50 ms (Studer et al., 1995). The frozen cultures with carriers were automatically ejected into a liquid nitrogen bath and prepared for cryosubstitution. Cryosubstitution of tissue water was performed using acetone (dried over calcium chloride) containing 2% osmium tetroxide, 0.12% water, and 0.1% uranylacetate. The samples were substituted at −90°C for 27 hours and for 8 hours each at −60°C and −30°C. The samples were then warmed to 4°C, washed three times for 10 minutes in 100% acetone, and embedded stepwise in Epon 812 (30%, 70%, 100% Epon). The blocks were polymerized at 60°C for 5 days.

Serial thin-sectioning for EM and 3D reconstruction of MF synapses

Thin sectioning was performed using a Leica EM UC6 (Leica). Serial thin sections (60 nm) were cut to allow for the complete reconstruction of individual MF synapses using the free and OpenSource software package OpenCAR developed by one of us (Kurt Saetzler; http://opencar.ulster.ac.uk; see Rollenhagen et al., 2007). Sections were placed on Formvar-coated copper slot grids and viewed in an LEO EM 906 E electron microscope.

In our EM analysis we focused on stratum lucidum of hippocampal region CA3, which was easily recognized by the bundles of thin preterminal MF axons and the giant MFBs just above the pyramidal cell layer (Fig. 1A). Digital micrographs of MFBs were taken at a primary magnification of 4,650× and stored as TIF images with a resulting pixel size of 2.5 nm. The electron microscopic images were imported into the reconstruction software OpenCAR, stacked, and transformed linearly such that corresponding structures were aligned along with all consecutive images comprising the 3D image stack of a MF synapse (for details, see Rollenhagen et al., 2007). In each image series comprising a 3D stack (two 3D stacks were analyzed with a total number of 170 micrographs), all structures of interest were marked, reconstructed, and analyzed as described. In order to measure vesicle diameter and cleft width for each bouton, 10 sections were randomly chosen from the set of sections spanning the bouton. The probability to pick a section was weighted by the area covered by the bouton. This increased the chance to see stretches of membrane that were cut almost perpendicularly and to find abundant vesicles in this section. The mean cleft width across a complete bouton was estimated by measuring the shortest 2D distance between pre- and postsynaptic traces that were directly apposing each other, and measurements were taken equidistantly along the bouton outline where pre- and postsynaptic membranes were clearly visible, indicating that they were cut almost perpendicularly. All calculations were performed offline using a batch version of OpenCAR, which generates 3D reconstructions as well as space delimited tables for each measurement which are readable by standard analysis software.

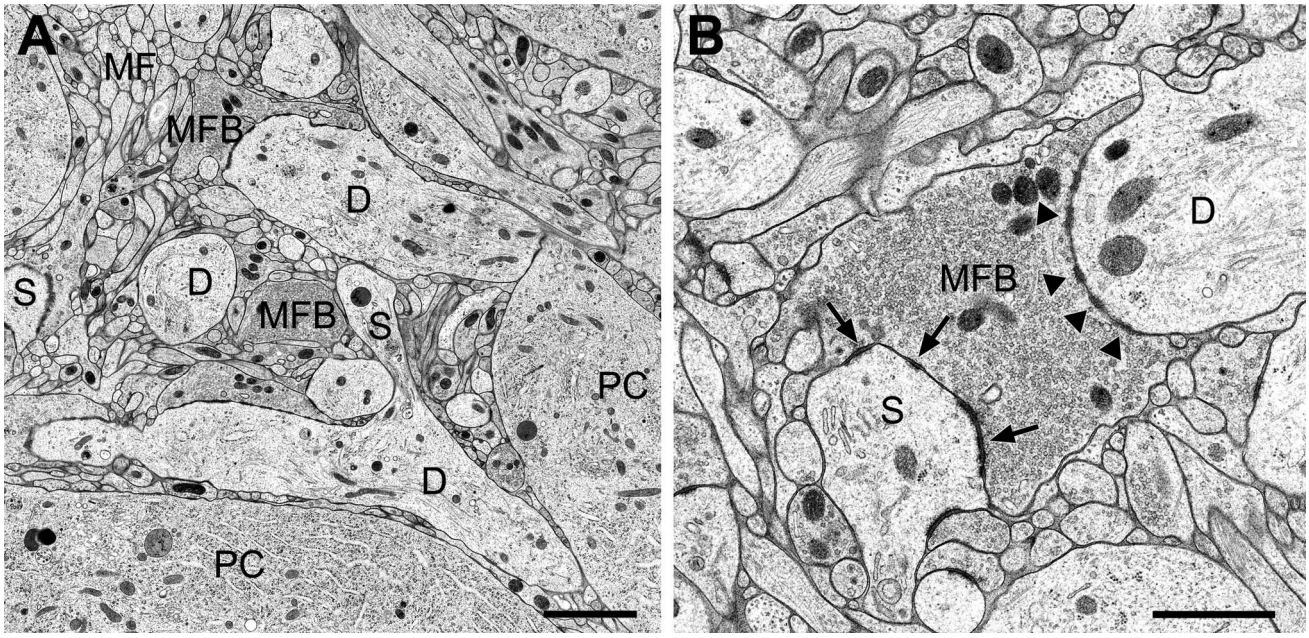

Figure 1. Fine structure of stratum lucidum of hippocampal region CA3 after high-pressure freezing (HPF). **A:** Low-power electron micrograph illustrating all major tissue components of CA3 such as cell bodies of pyramidal neurons (PC), proximal pyramidal cell dendrites (D) that give rise to large complex spines (S) in contact with mossy fiber boutons (MFBs), and bundles of unmyelinated preterminal mossy fibers (MFs). **B:** High-power electron micrograph of an MFB forming synaptic contacts (arrows) with a large complex spine (S). Arrowheads label nonsynaptic puncta adhaerentia with a dendritic shaft (D). Scale bars = 1 μm.

Quantitative EM analysis of cLTP-induced changes at MF synapses

Random sections through MFB profiles in wildtype control slice cultures (wt-con), wildtype TEA-treated cultures (wt-TEA), Munc13-1 knockout control cultures (m13-con), and Munc13-1 knockout cultures treated with TEA (m13-TEA) were used for these studies. To avoid double measurements, at least 3 μm of the block were sectioned before the next MFB profile was analyzed. In addition to their characteristic large size, MFB profiles were identified by their multiple (at least two) contacts with complex spines (Fig. 1A,B). MFB profiles ($n = 50$ for each experimental condition) were subjected to the following measurements using Analysis from Soft Imaging Software (SIS, Münster, Germany): Total number of vesicles, area and perimeter of MFB profile, number and length of active zones, number and area of spine profiles contacted by the MFB. From these data the density of synaptic vesicles (number of vesicles/μm^2 MFB area), the form factor MFB perimeter/MFB area, the number of active zones/μm^2 MFB area, and area of spine profiles/MFB area were calculated.

Digital Images

Digital images were captured using SIS software and stored as TIF images. Minimal adjustments to image brightness and contrast were made in Photoshop CS (v. 7.0; Adobe, San Jose, CA).

Statistics

Data are presented as mean ± SD; for statistical analysis a two-sided Student's *t*-test was applied ($\alpha = 0.05$). For electrophysiological data statistical significance was measured using Prism 5.0 software (GraphPad, San Diego, CA), applying the Wilcoxon signed rank test for paired data not normally distributed.

Levels of significance are indicated in the figures as $^*P < 0.05$, $^{**}P < 0.01$, and $^{***}P < 0.001$.

RESULTS

Fine structure of MF synapses after HPF

All structural characteristics of MF synapses, such as the giant presynaptic boutons densely filled with clear synaptic vesicles intermingled with a few dense-core vesicles and the synaptic contacts (active zones) with thorny excrescences on proximal CA3 pyramidal cell dendrites, were retained in slice cultures subjected to HPF in the absence of aldehyde fixatives (Fig. 1A,B). We conclude that HPF of hippocampal MF synapses resulted in the preservation of fine-structural detail of this synapse type. Moreover, 3D reconstruction of individual, HPF MF synapses from complete series of thin sections by using

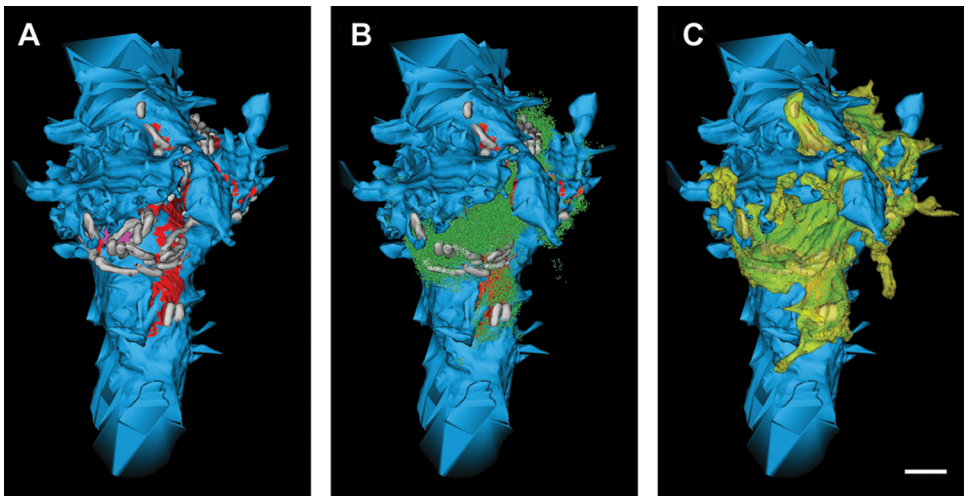

Figure 2. Complete 3D reconstruction of a mossy fiber bouton and its postsynaptic dendrite after HPF. **A–C:** Representative sequential frames from Video S1 showing the dendritic shaft and large complex spines (thorny excrescences) in blue, synaptic contacts in red, puncta adhaerentia in magenta, synaptic vesicles in green, mitochondria in white, and the dimensions of the presynaptic MFB in yellow. Scale bar = 1 μm.

TABLE 1.
Quantitative Analysis of Structural Components of Mossy Fiber Synapses After High-Pressure Freezing and After Perfusion Fixation

			HPF 01	HPF 03	Mean P 28	Mean adult
Bouton	Volume	[μm^3]	4.9	17.4	7.1	8.2
	Contact area with dendrite	[μm^2]	11.4	58.5	32.8	22.1
	Percentage of total contact area	%	35.9	44.7	44.4	37.6
Synaptic vesicles	Number per bouton		10656	39408	25133	15749
	Mean vesicle diameter	[nm]	29.6	29.0	31.7	31.2
	SD diameter	[nm]	4.4	4.2	6.0	5.0
Dense-core vesicles	Number per bouton		117	559	153	176
	Mean vesicle diameter	[nm]	56.1	58.7	67.7	62.4
	SD diameter	[nm]	7.3	7.4	14.1	11.6
Mitochondria	Number per bouton		11	59	29.5	29.5
	Total volume	[μm^3]	0.3	1.4	0.8	0.6
	Percentage of bouton volume	%	6.1	8.1	11.0	8.8
Cleft height	Mean	[nm]	18.0	15.6	25.6	20.3
	SD	[nm]	4.3	6.2	0.6	1.2
Active zones	Number per bouton		24	127	29.75	18.25
	Total area	[μm^2]	3.5	16.0	3.3	2.1
	Percentage of dendritic contact	%	30.4	27.3	10.2	9.7
	Mean area of active zone	[μm^2]	0.145	0.126	0.120	0.110
	SD area	[μm^2]	0.129	0.082	0.100	0.070

Measurements were performed in 3D reconstructions of two HPF-fixed mossy fiber synapses (HPF 01, HPF 03). For comparison data of perfusion-fixed young (P 28) and adult (3–4 months old) Wistar rats from a previous study are shown in which the same quantitative approach was used (Rollenhagen et al., 2007).

the software OpenCAR allowed for a description of the various components of this synapse in quantitative terms (Fig. 2; Supporting Video S1; Table 1). Interestingly enough, a comparison of the present quantitative data obtained in HPF mouse slice cultures did not reveal major differences to our previously published data in perfusion-fixed tissue from young and adult rats; however, the results showed variability of some synaptic structures (Table 1). Thus, the difference in total MFB volume was larger between the two completely reconstructed HPF boutons in slice cultures than between these and the two reconstructed MFBs in perfusion-fixed tissue. Interestingly enough, the percentage of contact area with dendritic structures turned out to be similar in the four reconstructed MFBs. The numbers of both clear synaptic vesicles and dense-core vesicles were large in the large HPF bouton (HPF 03), suggesting that the number of vesicles varied with bouton size. Similar observations

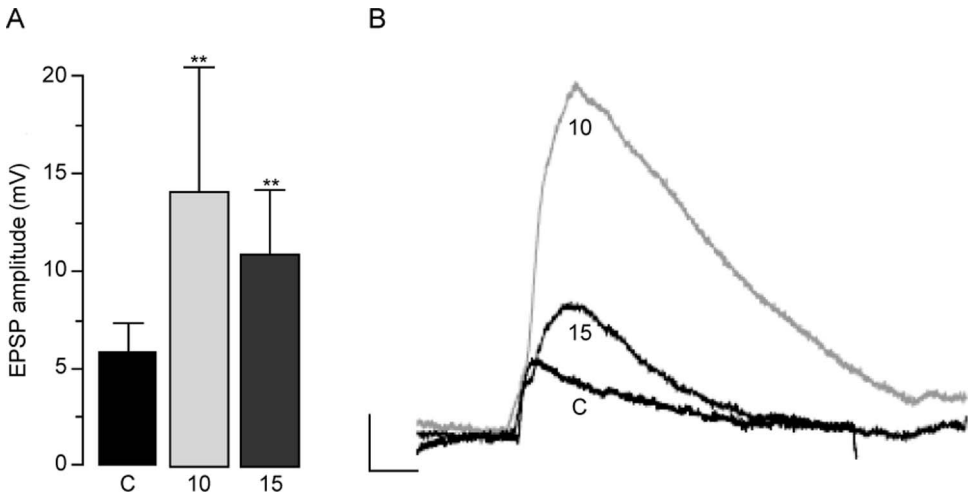

Figure 3. Analysis of EPSP amplitude induced by cLTP. **A:** Mean amplitude of EPSP under control condition (C, black bar), 10 minutes after TEA treatment (10, light gray bar), and 15 minutes after TEA treatment (15, dark gray bar). **B:** Measured EPSPs of a single CA3 pyramidal neuron before (C), 10 minutes (10), and 15 minutes (15) after cLTP induction. Data expressed as mean ± SD; $^{**}P < 0.01$ (Wilcoxon signed rank test). Scale bars = 25 ms and 5 mV, respectively.

were made with respect to the number and total area of active zones, whereas the mean area of active zones was similar in the four boutons analyzed. The mean vesicle diameter, a parameter assumed to be affected by dehydration in chemically fixed tissue, turned out to be similar in vesicles of perfusion-fixed rats and slice cultures subjected to HPF, and also the width of the synaptic cleft did not show major differences (Table 1). We conclude from these data that previous quantitative studies in perfusion-fixed MFBs (e.g., Rollenhagen et al., 2007) revealed reliable results and that shrinkage of synaptic components associated with chemical fixation and ethanol dehydration might have been overestimated.

Activity-induced increase in MFB membrane length

Based on the assumption that chemical LTP affects virtually all potentiatable synapses in the cultures, in contrast to activation of an indeterminate number of presynaptic fibers by electrical stimulation (Hosokawa et al., 1995), we induced LTP by brief (10 minutes) exposure of the slices to 25 mM TEA. Previous electrophysiological studies using a similar protocol have shown that robust LTP is induced under these conditions (Suzuki and Okada, 2008). Indeed, when we recorded from CA3 pyramidal neurons, first under control conditions and then after 10 minutes exposure to TEA, we observed strong potentiation of EPSPs (Fig. 3). While still being in the TEA solution, the cultures were directly subjected to HPF. Control cultures were not exposed to TEA; the investigator was blind to either treatment.

Following TEA treatment, we observed numerous small, omega-shaped invaginations of the presynaptic membrane of MFBs, likely representing the fusion or endocytotic recycling of synaptic vesicles (Fig. 4A). These invaginations were not only observed at synaptic sites but were also seen at nonsynaptic membrane segments. Of note, the MFB illustrated in Figure 4A likely impinges on a smooth dendritic shaft lacking excrescences. Contacts of MFBs with dendritic shafts are known to represent synapses with interneurons (Frotscher, 1985, 1989; Acsady et al., 1998). We reasoned that TEA stimulation would result in the fusion of many vesicles and thus counted the number of synaptic vesicles per bouton area. Indeed, the number of vesicles/μm^2 MFB area was significantly decreased in MFBs of TEA-treated cultures when compared with control cultures (TEA: 104 ± 43 SD; control: 183 ± 76 SD; $P = 0.000015$; Fig. 6A). While no statistically significant differences were found between TEA-treated and control cultures in the MFB area ($P = 0.851$), the ratio of MFB perimeter / MFB area, a value describing MFB shape, was significantly increased in TEA-treated cultures (TEA: 6.05 ± 1.52 SD; control: 3.85 ± 1.15 SD; $P = 0.00000018$; Fig. 6B), indicating an increase in length and a more labyrinthine course of the presynaptic membrane, likely resulting from numerous fusion events.

Close association of presynaptic and postsynaptic changes at MF synapses

Thorough analysis of numerous electron micrographs did not provide evidence for an increased dissociation of presynaptic and postsynaptic membranes resulting from

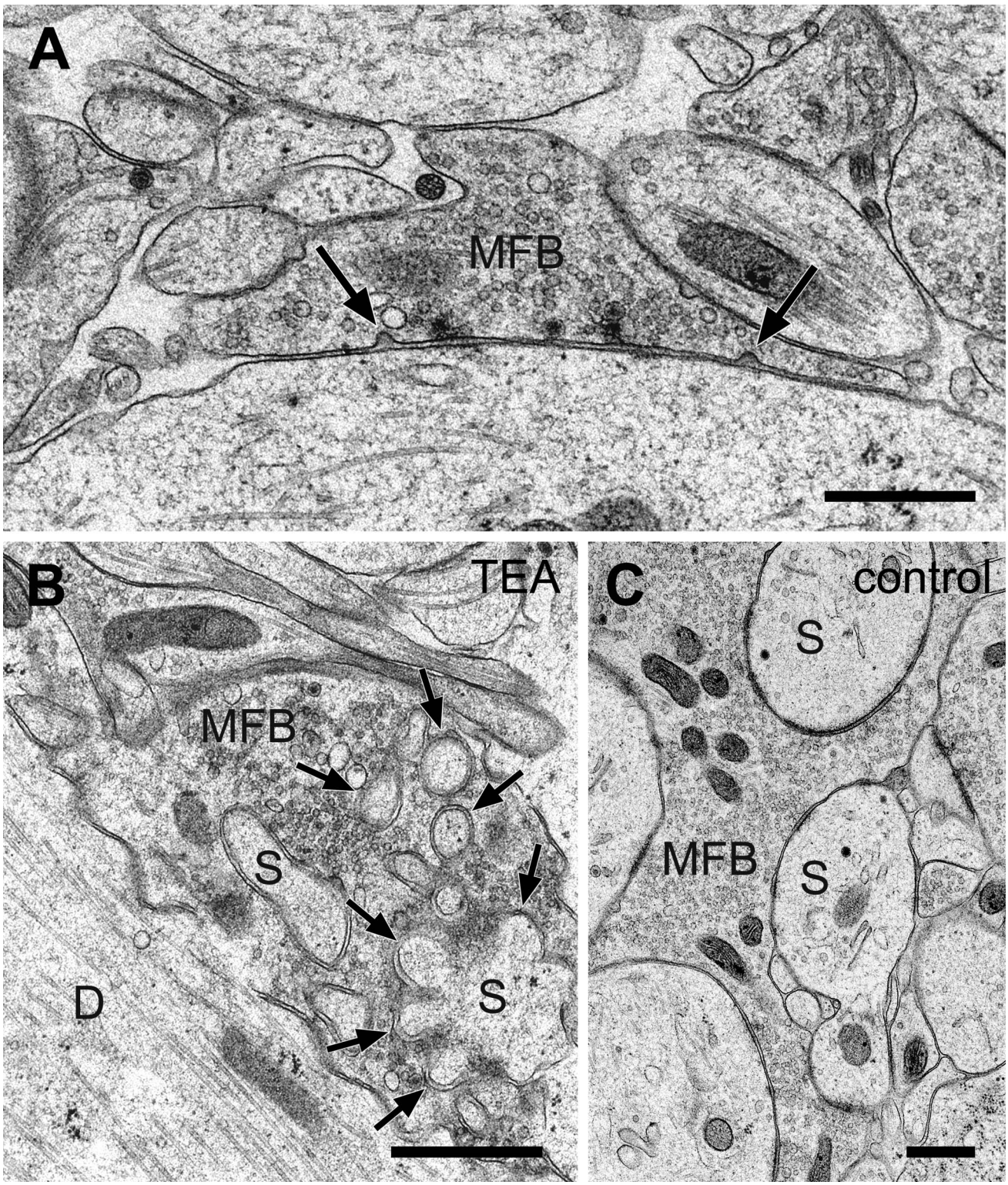

Figure 4. Structural changes at mossy fiber synapses after induction of cLTP. **A:** Following induction of cLTP (stimulation with TEA), MFBs show abundant membrane invaginations (arrows), probably representing fusion of synaptic vesicles with the presynaptic membrane or endocytotic vesicle recycling. **B:** Following induction of cLTP, the large spines (S) postsynaptic to MFBs give rise to small finger-shaped extensions (arrows). D, dendritic shaft. **C:** In control slice cultures, the large spines (S) show smooth contours, lacking the finger-like protrusions. Scale bars = 0.5 μm.

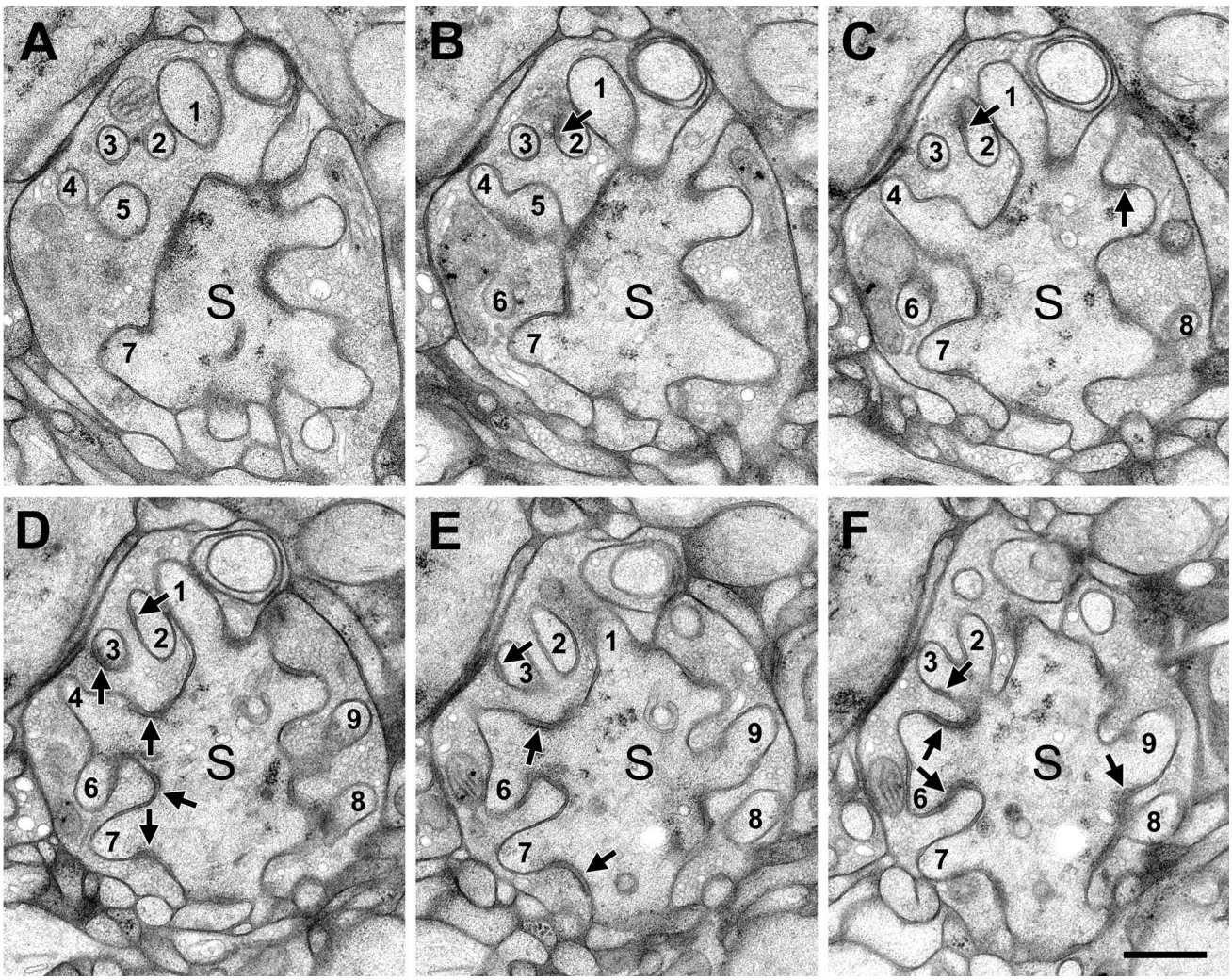

Figure 5. Serial reconstruction of finger-like protrusions from a complex spine after induction of cLTP. **A–F:** Mossy fiber bouton in contact with a complex spine (S) that gives rise to finger-like extensions (1–9). Synaptic contacts are labeled by arrows. Scale bar = 0.5 μm.

the more convoluted course of presynaptic membranes in TEA-stimulated MF synapses. Instead, likely associated with this convoluted shape of the presynaptic membrane, postsynaptic spines appeared more complex, with many finger-like extensions protruding into the presynaptic bouton when compared with their smooth, round structure in control cultures (Fig. 4B,C). Serial reconstructions of these finger-like protrusions clearly showed that they emerged from the thorny excrescences and were not fine perisynaptic glial processes (Fig. 5). Of note, synaptic contacts (active zones) were rarely seen at the top of the fingers but were found at their bases, often on both sides of the finger-like extension (Fig. 5). These contacts appeared shorter than synaptic contacts in nonstimulated cultures. The finger-like protrusions thus resembled the spinules of other synapse types. Quantitative analyses of spines that were completely embedded in the MFB in randomly chosen sections revealed a remarkable, statistically significant increase in the number of spine profiles/μm^2 MFB area, and also the area of spine profiles/MFB area was significantly increased (number of spines/μm^2 MFB area, TEA: 4.32 $\pm$ 2.19 SD; control: 0.42 $\pm$ 0.54 SD; $P = 1.569 \times 10^{-10}$; Fig. 6C; spine area/MFB area, TEA: 0.227 $\pm$ 0.078 SD; control: 0.134 $\pm$ 0.043 SD; $P = 0.0173$; Fig. 6D), likely representing the formation of the filopodial extensions observed after cLTP. The number of active zone profiles was increased following TEA stimulation (TEA: 3.63 $\pm$ 1.42 SD; control: 2.64 $\pm$ 1.21 SD; $P = 0.00882$; Fig. 6E); however, they were reduced in length (TEA: 168.69 nm $\pm$ 28.63 nm SD; control: 221.8 nm $\pm$ 75.04 SD; $P = 0.04031$; Fig. 6F), consistent with the notion that the size of the postsynaptic density is correlated with the dimensions of the spine head (Harris et al., 1992). We conclude that CA3

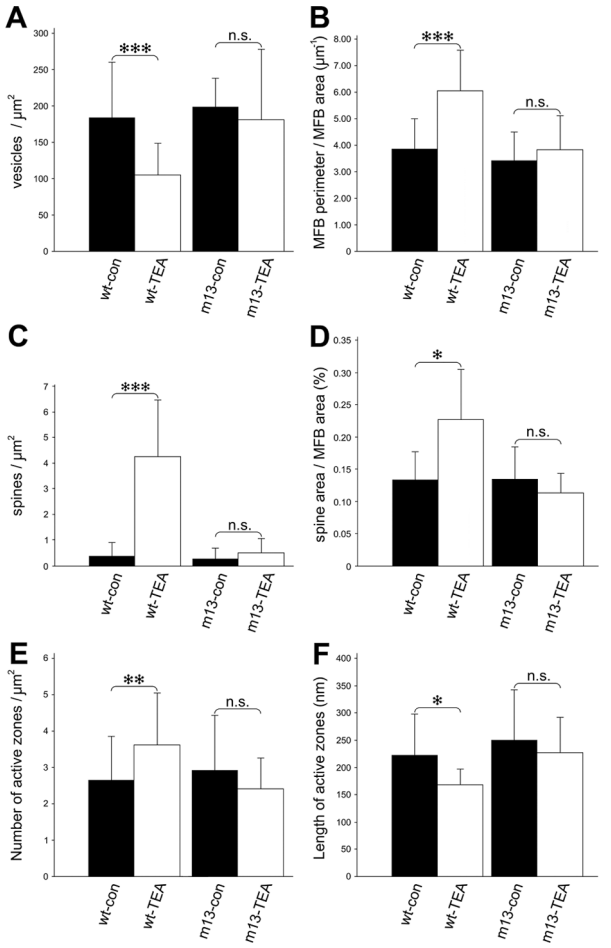

Figure 6. Quantitative structural changes at mossy fiber synapses induced by cLTP. **A:** Quantification of the number of synaptic vesicles/µm^2 MFB area. **B:** Ratio of MFB perimeter/MFB area. **C:** Number of spines/µm^2 MFB area. **D:** Ratio of spine area/MFB area. **E:** Number of active zones/µm^2 bouton area. **F:** Length of active zones in wildtype control cultures (wt-con), wildtype cultures treated with TEA to induce cLTP (wt-TEA), Munc13-1 knockout control cultures (m13-con), and Munc13-1 knockout cultures treated with TEA (m13-TEA). Data expressed as mean ± SD; ***$P < 0.001$; *$P < 0.05$ (two-sided *t*-test); n.s., not significant.

pyramidal cell spines change their shape by forming small protrusions in close association with an enlargement of the presynaptic MFB membrane.

Absence of MF synapse remodeling in Munc13-1 mutants

In Munc13-1 knockout mice, priming and fusion of synaptic vesicles is almost completely impaired (Augustin et al., 1999). We used hippocampal slice cultures of these mutant animals as a control for the observed structural changes in wildtype cultures after cLTP. Careful inspection of the fine structure of HPF MF synapses in Munc13-1 knockout cultures did not reveal abnormalities when compared with wildtype cultures. However, when Munc13-1 knockout cultures were exposed to TEA using the same protocol as for wildtype cultures, no significant decrease in the number of vesicles/µm^2 MFB area was observed (Munc13-1 control: 198 ± 39 SD; Munc13-1 TEA: 177 ± 95 SD; $P = 0.245$; Fig. 6A), likely because of the compromised vesicle priming in the absence of Munc13-1. Moreover, the shape of MFBs as determined by the ratio of MFB perimeter / MFB area was not altered in Munc13-1 knockout cultures treated with TEA as compared with untreated Munc13-1 knockout control cultures (Munc 13-1 TEA: 3.84 ± 1.31 SD; Munc13-1 control: 3.42 ± 1.08 SD; $P = 0.196$; Fig. 6B), and the spines postsynaptic to MFBs showed their normal, round appearance as seen in untreated Munc13-1 knockout cultures and wildtype cultures. No statistically significant differences were observed when the number and area of spines per MFB area were compared between TEA-treated and control cultures from Munc13-1 mice (number of spines/MFB area, Munc13-1, TEA: 0.57 ± 0.54 SD; Munc13-1 control: 0.32 ± 0.40 SD; $P = 0.1197$; spine area/MFB area, Munc13-1, TEA: 0.113 ± 0.030 SD; Munc13-1 control: 0.135 ± 0.051 SD; $P = 0.3573$; Fig. 6C,D). Also, the number and length of active zones were not significantly different (number of active zones/µm^2, Munc13-1, TEA: 2.41 ± 0.85 SD; Munc13-1 control: 2.92 ± 1.52 SD; $P = 0.9521$; Fig. 6E; length of active zones, Munc13-1, TEA: 227.62 nm ± 64.45 nm SD; Munc13-1 control: 250.33 nm ± 92.1 nm SD; $P = 0.4141$; Fig. 6F). The absence of significant changes in TEA-treated MFBs from Munc13-1 knockout mutants led us to conclude that the changes in vesicle density and presynaptic membrane length observed in wildtype tissue were due to increased vesicle fusions induced by cLTP.

DISCUSSION

HPF of slice cultures preserves fine-structural detail of MF synapses

The results of this study demonstrate that HPF of brain slice cultures is a useful approach to study structure–function relationships at identified central synapses. Not only were fine structural details of MF synapses well preserved after HPF, also cLTP-induced changes in the shape of presynaptic and postsynaptic structure could be monitored with this approach. Thus, an increase in presynaptic membrane length associated with remodeling of postsynaptic spine structure was captured at high resolution.

The principal characteristics of MF synapses on CA3 pyramidal neurons have long been known (Blackstad and Kjaerheim, 1961; Hamlyn, 1962). They were similarly observed in the present study employing HPF and

cryosubstitution. Thus, the thin unmyelinated axons of MFs gave rise to giant presynaptic boutons (MFBs) that terminated on proximal dendritic portions of CA3 pyramidal cells. They established characteristic synapses with large complex spines or thorny excrescences of CA3 pyramidal cells and with dendritic shafts of inhibitory interneurons (Blackstad and Kjaerheim, 1961; Hamlyn, 1962; Frotscher, 1985, 1989; Acsady et al., 1998). MFBs were densely filled with clear synaptic vesicles intermingled with a few dense-core vesicles. Up to 45 synaptic contacts (release sites) were established by a single MFB (Chicurel and Harris, 1992; Rollenhagen et al., 2007), and several synaptic contacts were formed on an individual spine. Nonsynaptic puncta adherentia were formed with the shafts of dendrites. While the synapses with interneurons serve feed-forward inhibition, the synapses with CA3 pyramidal cells are assumed to function as detonator synapses when activated repetitively (Henze et al., 2002). The MF projection to hippocampal region CA3 is assumed to be involved in the storage and recall of information and pattern completion (Bischofberger et al., 2006; Kerr and Jonas, 2008).

Rapid freezing of biological samples has been used previously to preserve ultrastructural detail that is lost in the process of aldehyde fixation and dehydration. In particular, attempts have been made to monitor the fusion of synaptic vesicles at neuromuscular junctions in response to neuronal activity by dropping the tissue on a cooled metal block (Heuser et al., 1979). A major problem of these initial studies has been the formation of ice crystals in portions of the tissue remote from the cooling surface. HPF has overcome these problems to a large extent because freezing under high pressure was found to increase vitrification depth more than 10-fold (Sartori et al., 1993). In spite of these advantages, application of HPF to the study of mammalian nervous tissue has remained difficult, and the few studies published so far have focused on specific biological questions (Rostaing et al., 2006; Siksou et al., 2007, 2009). The limited use of HPF for studies of mammalian central nervous system (CNS) tissue is due to the fact that fresh samples of brain tissue cannot be removed without uncontrolled damage to neurons and their long axonal and dendritic processes. Here we used hippocampal slice cultures that were incubated for 2 weeks to allow for recovery of the tissue from damage associated with culture preparation. Under these conditions slice cultures have proven to preserve "organotypic" characteristics of the tissue such as a region-specific organization of the extracellular matrix and cell type-specific features including the formation of specific synaptic connections such as the MF–CA3 neuron synapse (Frotscher and Gähwiler, 1988; Gähwiler et al., 1997).

cLTP-induced spine growth is linked to growth of presynaptic MFBs

The present results suggest increased vesicle fusions associated with changes in the shape of MFBs. Similar changes were not observed in MFBs of Munc13-1 knockout mice in which synaptic vesicle priming and fusion are blocked (Augustin et al., 1999). We conclude that we captured a fusion-induced increase in the length of the presynaptic membrane in the wildtype cultures.

The described elongation of MFB membrane was accompanied by several other interesting observations. Despite the more convoluted course of the presynaptic membrane, there was no indication of a dissociation of presynaptic and postsynaptic structures. Rather, finger-like protrusions of postsynaptic spines seemed to follow the labyrinthine course of the MFB membrane. It has long been known that pre- and postsynaptic membranes establish strong mechanical contact (Gray and Whittaker, 1962), likely by the abundance of cell adhesion molecules at synaptic sites (Washbourne et al., 2004; Hortsch and Umemori, 2009). It thus appeared that the postsynaptic spine changed its shape in response to an increase in MFB membrane length. Along this line, there was a significant increase in the number of small filopodial spines with short active zones in cLTP. Several studies have shown that LTP induction results in the formation and growth of dendritic spines in hippocampal region CA1 (Engert and Bonhoeffer, 1999; Yuste and Bonhoeffer, 2001; Matsuzaki et al., 2004; Yang et al., 2008). An increase in the size and complexity of spines may underlie the maintenance of LTP and memory consolidation since the number of functional glutamate receptors increases with spine size (Matsuzaki et al., 2001; Noguchi et al., 2005; Beique et al., 2006; Zito et al., 2009; Kasai et al., 2010). Of note, the increase in the number of small spines postsynaptic to MFBs described here was not observed in Munc13-1 mutant mice. One interpretation of our findings is that mechanical force initiated by presynaptic membrane folding and mediated to the postsynaptic element via synapse-associated adhesion molecules contributes to activity-induced growth and reorganization of the postsynaptic element, including remodeling of the actin cytoskeleton (Fischer et al., 1998, 2000; Star et al., 2002; Fukazawa et al., 2003; Okamoto et al., 2004; Hotulainen et al., 2009). The lack of changes in postsynaptic spines in MF synapses from Munc13-1 mutants would accordingly point to an inductive role of the presynaptic element in the formation of new spines, as was concluded some time ago from deafferentation experiments (Hámori, 1973; Frotscher et al., 1977). Such a scenario would be compatible with presynaptic LTP expression at this particular synapse (Nicoll and

Schmitz, 2005). However, the present results do not exclude direct effects of TEA-induced glutamate release on postsynaptic spines.

ACKNOWLEDGMENT

The authors thank Professor Peter Jonas for helpful comments on the article.

LITERATURE CITED

Acsady L, Kamondi A, Sik A. Freund T, Buzsaki G. 1998. GABAergic cells are the major postsynaptic targets of mossy fibers in the rat hippocampus. J Neurosci 18: 3386–3403.

Augustin I, Rosenmund C, Südhof TC, Brose N. 1999. Munc13–1 is essential for fusion competence of glutamatergic synaptic vesicles. Nature 400:457–461.

Bailey CH, Kandel ER. 1993. Structural changes accompanying memory storage. Annu Rev Physiol 55:397–426.

Beique JC, Lin DT, Kang MG, Aizawa H, Takamiya K, Huganir RL. 2006. Synapse-specific regulation of AMPA receptor function by PSD-95. Proc Natl Acad Sci U S A 103: 19535–19540.

Bischofberger J, Engel D, Frotscher M, Jonas P. 2006. Timing and efficacy of transmitter release at mossy fiber synapses in the hippocampal network. Pflügers Arch Eur J Physiol 453:361–372.

Blackstad TW, Kjaerheim A. 1961. Special axodendritic synapses in the hippocampal cortex: electron and light microscopic studies on the layer of mossy fibers. J Comp Neurol 117:113–159.

Bliss TVP, Collingridge GL. 1993. A synaptic model of memory: long-term potentiation in the hippocampus. Nature 361:31–39.

Bliss T, Collingridge G, Morris R. 2007. Synaptic plasticity in the hippocampus. In: Andersen P, Morris R, Amaral D, Bliss T, O'Keefe J, editors. The hippocampus book. New York: Oxford University Press. p 343–474.

Buchs PA, Muller D. 1996. Induction of long-term potentiation is associated with major ultrastructural changes of activated synapses. Proc Natl Acad Sci U S A 93:8040–8045.

Chicurel ME, Harris KM. 1992. Three-dimensional analysis of the structure and composition of CA3 branched dendritic spines and their synaptic relationships with mossy fiber boutons in the rat hippocampus. J Comp Neurol 325: 169–182.

Emptage NJ, Reid CA, Fine A, Bliss TVP. 2003. Optical quantal analysis reveals a presynaptic component of LTP at hippocampal Schaffer-associational synapses. Neuron 38: 797–804.

Engert F, Bonhoeffer T. 1999. Dendritic spine changes associated with hippocampal long-term synaptic plasticity. Nature 399:66–70.

Fischer M, Kaech S, Knutti D, Matus A. 1998. Rapid actin-based plasticity in dendritic spines. Neuron 20:847–854.

Fischer M, Kaech S, Wagner U, Brinkhaus H, Matus A. 2000. Glutamate receptors regulate actin-based plasticity in dendritic spines. Nat Neurosci 3:887–894.

Frotscher M. 1985. Mossy fibres form synapses with identified pyramidal basket cells in the CA3 region of the guinea pig hippocampus: a combined Golgi-electron microscope study. J Neurocytol 14:245–259.

Frotscher M. 1989. Mossy fiber synapses on glutamate decarboxylase-immunoreactive neurons: evidence for feed-forward inhibition in the CA3 region of the hippocampus. Exp Brain Res 75:441–445.

Frotscher M, Gähwiler BH. 1988. Synaptic organization of intracellularly stained CA3 pyramidal neurons in slice cultures of rat hippocampus. Neuroscience 24:541–551.

Frotscher M, Hámori J, Wenzel J. 1977. Transneuronal effects of entorhinal lesions in the early postnatal period on synaptogenesis in the hippocampus of the rat. Exp Brain Res 30:549–560.

Fukazawa Y, Saitoh Y, Ozawa F, Ohta Y, Mizuno K, Inokuchi K. 2003. Hippocampal LTP is accompanied by enhanced F-actin content within the dendritic spine that is essential for late LTP maintenance in vivo. Neuron 38:447–460.

Gähwiler BH, Capogna M, Debanne D, McKinney RA, Thompson SM. 1997. Organotypic slice cultures: a technique has come of age. Trends Neurosci 20:471–477.

Galimberti I, Gogolla N, Alberi S, Santos AF, Muller D, Caroni P. 2006. Long-term rearrangements of hippocampal mossy fiber terminal connectivity in the adult regulated by experience. Neuron 50:749–763.

Galimberti I, Bednarek E, Donato F, Caroni P. 2010. EphA4 signaling in juveniles establishes topographic specificity of structural plasticity in the hippocampus. Neuron 65:627–642.

Geinisman Y. 2000. Structural synaptic modifications associated with hippocampal LTP and behavioral learning. Cereb Cortex 10:952–962.

Gray EG, Whittaker VP. 1962. The isolation of nerve endings from brain: an electron-microscope study of cell fragments derived by homogenization and centrifugation. J Anat (Lond) 96:79–80.

Hamlyn LH. 1962. The fine structure of the mossy fibre endings in the hippocampus of the rabbit. J Anat 97:112–120.

Hámori J. 1973. The inductive role of presynaptic axons in the development of postsynaptic spines. Brain Res 62:337–344.

Harris EW, Cotman CW. 1986. Long-term potentiation of guinea pig mossy fiber responses is not blocked by N-methyl D-aspartate antagonists. Neurosci Lett 70:132–137.

Harris KM, Jensen FE, Tsao B. 1992. Three-dimensional structure of dendritic spines and synapses in rat hippocampus (CA1) at postnatal day 15 and adult ages: implications for the maturation of synaptic physiology and long-term potentiation. J Neurosci 12:2685–2705.

Harris KM, Fiala JC, Ostroff L. 2003. Structural changes at dendritic spine synapses during long-term potentiation. Philos Trans R Soc Lond B 358:745–748.

Hebb DO. 1949. The organization of behaviour. New York: John Wiley & Sons.

Henze DA, Wittner L, Buzsaki G. 2002. Single granule cells reliably discharge targets in the hippocampal CA3 network in vivo. Nat Neurosci 5:790–795.

Heuser JE, Reese TS, Dennis MJ, Jan Y, Jan L, Evans L. 1979. Synaptic vesicle exocytosis captured by quick freezing and correlated with quantal transmitter release. J Cell Biol 81: 275–300.

Hortsch M, Umemori H (eds.). 2009. The sticky synapse. Berlin: Springer.

Hosokawa T, Rusakov DA, Bliss TVP, Fine A. 1995. Repeated confocal imaging of individual dendritic spines in the living hippocampal slice: evidence for changes in length and orientation associated with chemically induced LTP. J Neurosci 15:5560–5573.

Hotulainen P, Hoogenraad CC. 2010. Actin in dendritic spines: connecting dynamics to function. J Cell Biol 189:619–629.

Hotulainen P, Llano O, Smirnov S, Tanhuanpää K, Faix J, Rivera C, Lappalainen P. 2009. Defining mechanisms of actin polymerization and depolymerization during dendritic spine morphogenesis. J Cell Biol 185:323–339.

Kasai H, Fukuda M, Watanabe S, Hayashi-Takagi A, Noguchi J. 2010. Structural dynamics of dendritic spines in memory and cognition. Trends Neurosci 33:121–129.

Kerr AM, Jonas P. 2008. The two sides of hippocampal mossy fiber plasticity. Neuron 57:5–7.

Kwon H-B, Castillo PE. 2008. Long-term potentiation selectively expressed by NMDA receptors at hippocampal mossy fiber synapses. Neuron 57:108–120.

Lauri SE, Palmer M, Segerstrale M, Vesikansa A, Taira T, Collingridge GL. 2007. Presynaptic mechanisms involved in the expression of STP and LTP at CA1 synapses in the hippocampus. Neuropharmacology 52:1–11.

Maletic-Savatic M, Malinow R, Svoboda K. 1999. Rapid dendritic morphogenesis in CA1 hippocampal dendrites induced by synaptic activity. Science 283:1923–1927.

Matsuzaki M, Ellis-Davies GCR, Nemoto T, Miyashita Y, Iino M, Kasai H. 2001. Dendritic spine geometry is critical for AMPA receptor expression in hippocampal CA1 pyramidal neurons. Nat Neurosci 4:1086–1092.

Matsuzaki M, Honkura N, Ellis-Davies GCR, Kasai H. 2004. Structural basis of long-term potentiation in single dendritic spines. Nature 429:761–766.

Matus, A. 2000. Actin-based plasticity in dendritic spines. Science 290:754–758.

Nicoll RA, Schmitz D. 2005. Synaptic plasticity at hippocampal mossy fibre synapses. Nat Rev Neurosci 6:863–876.

Nicoll RA, Kauer JA, Malenka RC. 1988. The current excitement in long-term potentiation. Neuron 1:97–103.

Noguchi J, Matsuzaki M, Ellis-Davies GCR, Kasai H. 2005. Spine-neck geometry determines NMDA receptor-dependent Ca^{2+} signaling in dendrites. Neuron 46:609–622.

Okamoto K-I, Nagai T, Miyawaki A, Hayashi Y. 2004. Rapid and persistent modulation of actin dynamics regulates postsynaptic reorganization underlying bidirectional plasticity. Nat Neurosci 7:1104–1105.

Ramón y Cajal SR. 1911. Histologie du système nerveux de l'homme et des vertébrés. Vol. II. Paris: Maloine.

Rebola N, Lujan R, Cunha RA, Mulle C. 2008. Adenosine A_{2A} receptors are essential for long-term potentiation of NMDA-EPSCs at hippocampal mossy fiber synapses. Neuron 57:121–134.

Rekart JL, Sandoval CJ, Bermudez-Rattoni F, Routtenberg A. 2007. Remodeling of hippocampal mossy fibers is selectively induced seven days after the acquisition of a spatial but not a cued reference memory task. Learn Mem 14: 416–421.

Rollenhagen A, Sätzler K, Rodriguez EP, Jonas P, Frotscher M, Lübke JHR. 2007. Structural determinants of transmission at large hippocampal mossy fiber synapses. J Neurosci 27: 10434–10444.

Rostaing P, Real E, Siksou L, Lechaire J-P, Boudier T, Boeckers TM, Gertler F, Gundelfinger ED, Triller A, Marty S. 2006. Analysis of synaptic ultrastructure without fixative using high-pressure freezing and tomography. Eur J Neurosci 24: 3463–3474.

Routtenberg A. 2010. Adult learning and remodeling of hippocampal mossy fibers: unheralded participant in circuitry for long-lasting spatial memory. Hippocampus 20:44–45.

Sartori N, Richter K, Dubochet J. 1993. Vitrification depth can be increased more than 10-fold by high-pressure freezing. J Microsc 172:55–61.

Segal M. 2005. Dendritic spines and long-term plasticity. Nat Rev Neurosci 6:277–284.

Siksou L, Rostaing P, Lechaire JP, Boudier T, Ohtsuka T, Fejtova A, Kao HT, Greengard P, Gundelfinger ED, Triller A, Marty S. 2007. Three-dimensional architecture of presynaptic terminal cytomatrix. J Neurosci 27:6868–6877.

Siksou L, Varoqueaux F, Pascual O, Triller A, Brose N, Marty S. 2009. A common molecular basis for membrane docking and functional priming of synaptic vesicles. Eur J Neurosci 30:49–56.

Star EN, Kwiatkowski DJ, Murthy VN. 2002. Rapid turnover of actin in dendritic spines and its regulation by activity. Nat Neurosci 5:239–246.

Stevens CF, Wang Y. 1994. Changes in reliability of synaptic function as a mechanism for plasticity. Nature 371:704–707.

Stoppini L, Buchs PA, Muller DA. 1991. A simple method for organotypic cultures of nervous tissue. J Neurosci Methods 37:173–182.

Studer D, Michel M, Wohlwend M, Hunziker EB, Buschmann M. 1995. Vitrification of articular cartilage by high-pressure freezing. J Microsc 179:321–332.

Studer D, Graber W, Al-Amoudi A, Eggli P. 2001. A new approach for cryofixation by high-pressure freezing. J Microsc 203:285–294.

Suzuki E, Okada T. 2008. TEA-induced long-term potentiation at hippocampal mossy fiber-CA3 synapses: characteristics of its induction and expression. Brain Res 1247:21–27.

Toni N, Buchs PA, Nikonenko I, Bron CR, Muller D. 1999. LTP promotes formation of multiple spine synapses between a single axon terminal and a dendrite. Nature 402:421–425.

Trachtenberg JT, Chen BE, Knott GW, Feng G, Sanes JR, Welker E, Svoboda K. 2002. Long-term in vivo imaging of experience-dependent synaptic plasticity in adult cortex. Nature 420:788–794.

Washbourne P, Dityatev A, Scheiffele P, Biederer T, Weiner JA, Christopherson KS, El-Husseini A. 2004. Cell adhesion molecules in synapse formation. J Neurosci 24:9244–9249.

Whitlock JR, Heynen AJ, Shuler MG, Bear MF. 2006. Learning induces long-term potentiation in the hippocampus. Science 313:1093–1097.

Yang Y, Wang X-b, Frerking M, Zhou Q. 2008. Spine expansion and stabilization associated with long-term potentiation. J Neurosci 28:5740–5751.

Yang G, Pan F, Gan WB. 2009. Stably maintained dendritic spines are associated with lifelong memories. Nature 462: 920–924.

Yuste R, Bonhoeffer T. 2001. Morphological changes in dendritic spines associated with long-term synaptic plasticity. Annu Rev Neurosci 24:1071–1089.

Zito K, Scheuss V, Knott G, Hill T, Svoboda K. 2009. Rapid functional maturation of nascent dendritic spines. Neuron 61:247–258.